

Effect of sintering temperature on structural and electrical properties of gadolinium doped ceria ($\text{Ce}_{0.9}\text{Gd}_{0.1}\text{O}_{1.95}$)

L D JADHAV*, S H PAWAR and M G CHOURASHIYA

Department of Physics, Shivaji University, Kolhapur 416 004, India

MS received 28 September 2006; revised 9 January 2007

Abstract. Gadolinium doped ceria oxide is one of the promising materials as an electrolyte for IT-SOFCs. $\text{Ce}_{0.9}\text{Gd}_{0.1}\text{O}_{1.95}$ (GDC10) powder was prepared by solid state reaction and sintered at 1473 K, 1573 K, 1673 K and 1773 K. All samples were studied using X-ray diffraction, scanning electron micrograph and d.c. conductivity measurement. The crystallinity and surface morphology of the samples improved with sintering temperature. Further, the electrical conductivity measurement indicated that the conduction mechanism is mainly ionic. The conductivity of samples sintered at 1673 K and 1773 K at 800°C are of the order of $0.1 \text{ S}\cdot\text{cm}^{-1}$. The activation energies decreased from 1.25–0.82 eV with increase in sintering temperature.

Keywords. $\text{Ce}_{0.9}\text{Gd}_{0.1}\text{O}_{1.95}$; IT-SOFC; XRD; SEM.

1. Introduction

Solid oxide fuel cells (SOFCs) are of two types based on their operating temperatures: high temperature SOFCs and low temperature or intermediate temperature SOFCs (i.e. IT-SOFCs). The problem encountered in commercializing HT-SOFC has motivated researchers to develop materials that could allow the SOFC operation at intermediate temperatures. Various groups around the world are involved in developing cathode, anode and electrolyte materials for IT-SOFC.

For IT-SOFC, the electrolyte material must have high ionic conductivity at comparatively lower temperature. The conventional YSZ ($\text{Y}_2\text{O}_3\text{-ZrO}_2$) electrolyte shows the required ionic conductivity (i.e. $0.1 \text{ S}\cdot\text{cm}^{-1}$) at 1000°C; hence, it requires a higher operating temperature. In order to reduce the operating temperature, two approaches are widely applied. The resistance of dense electrolyte membranes is decreased by decreasing thickness of the traditional YSZ electrolyte or using alternative materials of higher ionic conductivity at comparatively lower temperatures (Mogensen *et al* 2000; Singhal 2000; Steele 2000a). Gadolinium-doped ceria (GDC) is one of the most promising electrolytes for SOFCs to be operated below 650°C (Sahibzada *et al* 2000; Steele 2000b; Zha *et al* 2001a, b). In view of the various advantages over the conventional electrolytes, YSZ and recently developed BICUMVOX material, we have planned to develop gadolinium doped ceria oxide as an electrolyte.

Various synthesis and processing methods have been used to prepare doped ceria with desired properties, in-

cluding hydrothermal synthesis (Hirano and Kato 1996), homogeneous precipitation (Herle *et al* 1996, 1997; Zha *et al* 2001c), sol-gel process (Huang *et al* 1997) and glycine-nitrate process (GNP) (Park *et al* 1997; Xia and Liu 2001a, b; Xia *et al* 2001). Further, solid-state reaction, a simple and cost-effective method, is often adopted to prepare bulk electrolyte samples (Wang *et al* 1998; Zhang *et al* 2003) and cathode materials (Gschneidner 1979; Qiu *et al* 2003).

In the present paper, we have prepared $\text{Ce}_{0.9}\text{Gd}_{0.1}\text{O}_{1.95}$ (GDC10) by ceramic route. The material is then sintered at different temperatures and the effect of sintering temperature on the structural, morphological and electrical properties is discussed in detail.

2. Experimental

Commercially available powders of CeO_2 (AR, 99.9% HIMEDIA; make) and Gd_2O_3 (AR grade, 99.9% HIMEDIA, make) were used as starting materials. The powders of CeO_2 and Gd_2O_3 were mixed in stoichiometric proportions to obtain GDC10 ($\text{Ce}_{0.9}\text{Gd}_{0.1}\text{O}_{1.95}$) compositions. The mixture was then homogenized by agate-mortar. The mixed powder was calcined at 1023 K for 2 h and reground with agate-mortar. The powder was then hardened with hydraulic press machine at a pressure of about 10–12 tons/sq-inch in circular disk shaped pellets for all samples. The samples were then sintered at 1473 K, 1573 K, 1673 K and 1773 K for 2 h in air and identified as GDC114, GDC115, GDC116 and GDC117, respectively. The heating rate was kept at 3 K/min and cooling rate was kept at 1 K/min for all samples.

The phase composition of the sintered GDC10 pellets was studied using X-ray diffraction (PW-3710) with Cu-K α .

*Author for correspondence (lata_phy@unishivaji.ac.in)

The surface morphology of the samples was revealed using scanning electron microscope (SEM, JEOL-JSM-6360). The d.c. electrical conductivity of the samples was studied by two-probe method.

3. Results and discussion

3.1 Structural characterization

Figure 1 shows XRD patterns of the samples sintered at different temperatures, i.e. GDC114, GDC115, GDC116 and GDC117. The XRD data obtained for all four samples was compared with the JCPDS file no. 750161. All the samples showed the presence of (111), (200), (220), (311), (222), (400), (331), (420) and (422) reflection peaks in the scanning range $20-90^\circ$ of 2θ . No impurity peaks were observed. This confirms the 'fcc' structure of prepared material.

The lattice parameter 'a' was calculated using the relation

$$a = d \cdot \sqrt{h^2 + k^2 + l^2}, \quad (1)$$

and depicted in figure 2. The lattice parameter, a , for the GDC114 is 5.4045 \AA , which increased to 5.4197 \AA for GDC115. Further increase in sintering temperature lowers the lattice parameter for both the GDC116 and GDC117

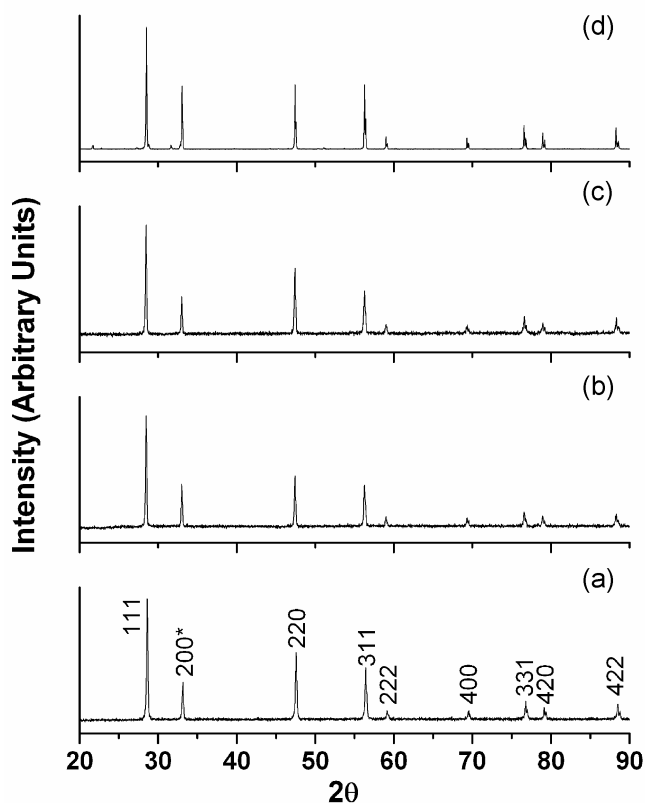


Figure 1. The XRD patterns of samples (a) GDC114, (b) GDC115, (c) GDC116 and (d) GDC117.

samples. The lattice parameter for GDC116 and GDC117 is 5.4185 \AA , which is in agreement with the reported value of 5.418 \AA (Brauer and Gradinger 1954). It is also found that relative intensity of the diffraction peak (200) increases with sintering temperature, indicating a good crystal orientation (Song *et al* 2003).

The crystallite size of the samples sintered at different temperatures were calculated using the Scherrer's equation

$$D = (0.9\lambda)/(\beta \cos\theta), \quad (2)$$

where β is the line broadening measured at half of height of peak, θ the angle of reflection and λ the radiation wavelength.

The calculated crystallite size is presented in figure 3. The size of crystallite is observed to improve with sintering temperature.

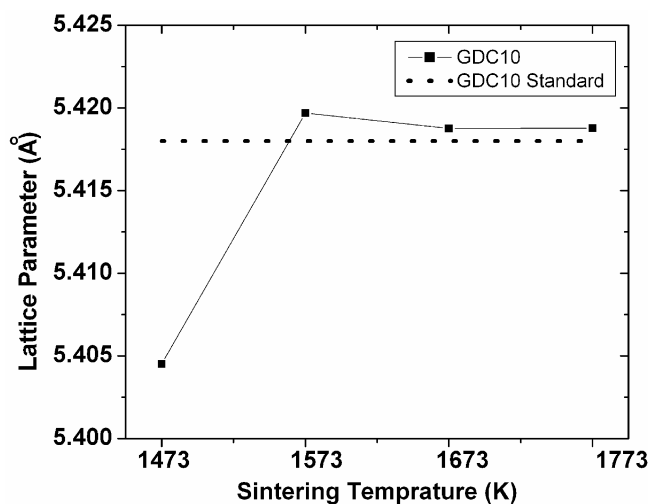


Figure 2. Variation in lattice parameter, a , of GDC10 sintered at different temperatures.

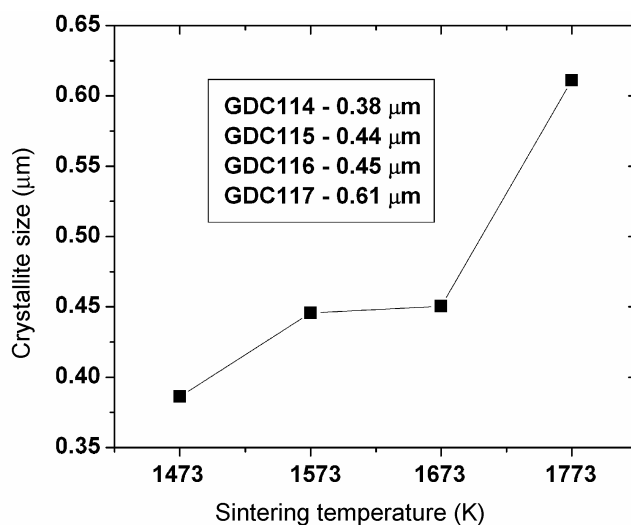


Figure 3. Variation in crystallite size for GDC10 samples as a function of sintering temperature.

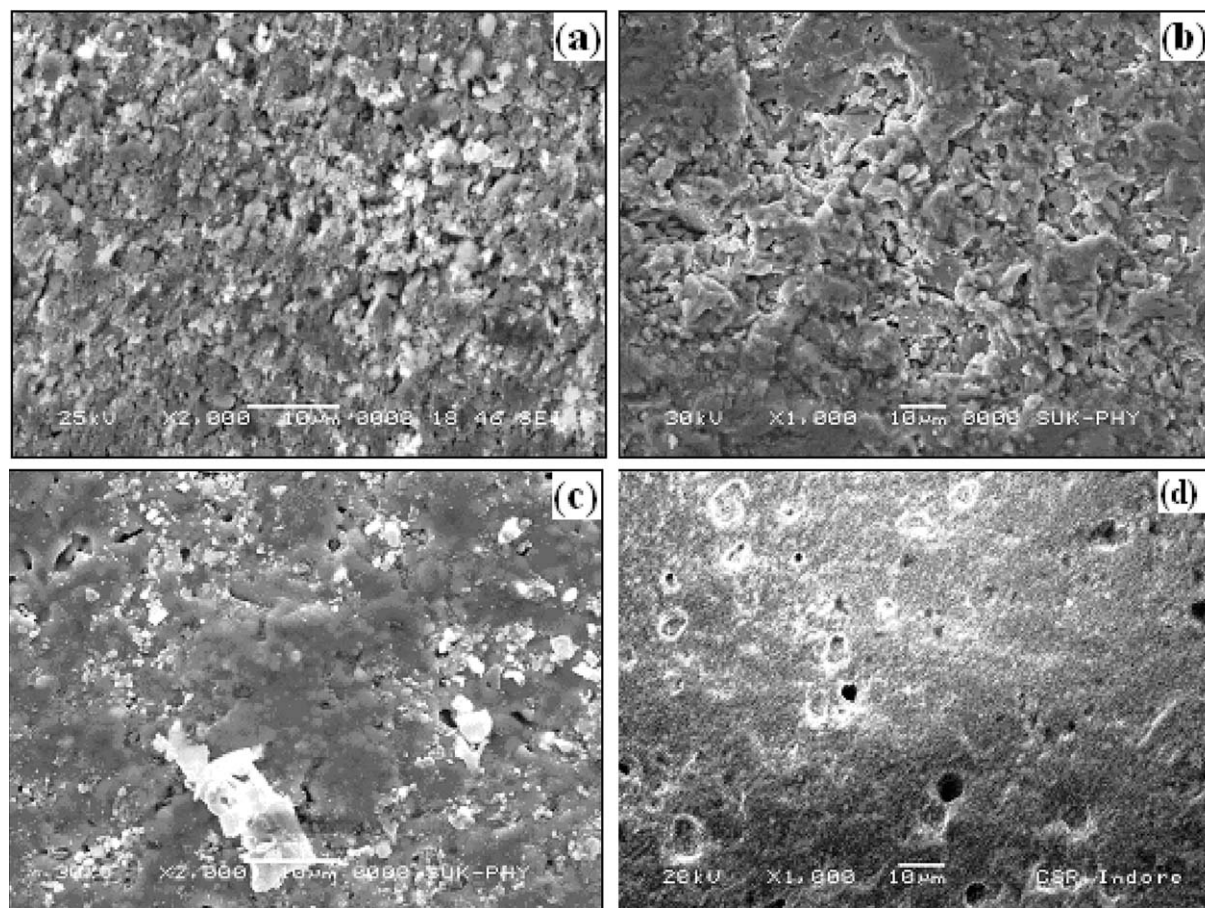


Figure 4. SEMs of samples: (a) GDC114, (b) GDC115, (c) GDC116 and (d) GDC117.

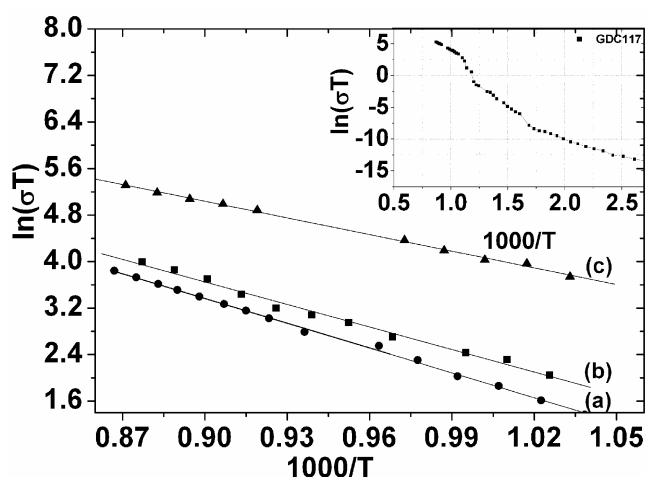


Figure 5. Variation of $\ln(\sigma T)$ with $1000/T$: (a) GDC115, (b) GDC116 and (c) GDC117. Inset shows the variation of $\ln(\sigma T)$ with $1000/T$ of GDC117 in the temperature range 75–855°C.

3.2 Morphological characterization

Figure 4 shows SEM of samples GDC114, GDC115, GDC116 and GDC117. The SEM of all four samples clearly rectifies the effect of sintering temperature on its surface morphology. The amount of porosity as well as size

of pores decreases as sintering temperature is increased. Also the surface gets modified and become smoother for higher sintering temperature. GDC117 is highly uniform and with no cracked surface.

The SEM at higher magnification gives direct estimation of grain size. The average grain size increased with sintering temperature and it being 0.75 μm , 2 μm , 2.5 μm and 3 μm for GDC114, GDC115, GDC116 and GDC117, respectively. This is consistent with XRD results.

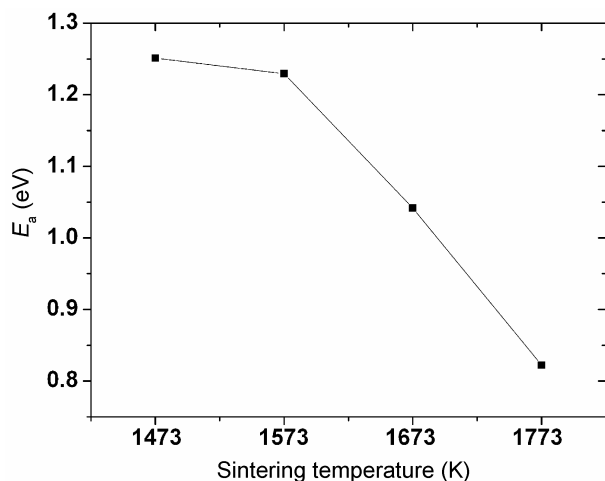
3.3 Conductivity measurement

The d.c. conductivity measurement was done by two-probe method in air in the temperature range 298–1123 K. The variation of $\ln(\sigma T)$ with $1000/T$ for the GDC10 pellets sintered at 1473 K, 1573 K, 1673 K and 1773 K showed the change in slope at around 300°C and 650°C (inset of figure 5 for GDC117). The change in slope at 300°C is attributed to initiation of ionic diffusion and that at 650°C may be due to slight change in mechanism of conduction (Zha *et al* 2003). Figure 5 shows the $\ln(\sigma T)$ vs $1000/T$ relation for GDC115, GDC116 and GDC117.

The conductivity at 800°C is tabulated in table 1. The conductivity of GDC117 at 800°C is 0.121 $\text{S}\cdot\text{cm}^{-1}$, which almost equals the value of YSZ at 1000°C (Chen *et al*

Table 1. The conductivities of samples GDC114, GDC115, GDC116 and GDC117 at 800°C.

Sample	Conductivity at 800°C (S-cm ⁻¹)
GDC114	0.64 × 10 ⁻³
GDC115	0.94 × 10 ⁻³
GDC116	0.91 × 10 ⁻³
GDC117	0.12

**Figure 6.** Variation of activation energy with sintering temperature.

2002) and slightly higher than the value of 0.118 S-cm⁻¹ reported by Zha *et al* (2003).

Activation energies (E_a) for conductivity data were calculated by fitting the data to the Arrhenius relation for thermally activated conduction which is given as

$$\sigma = (\sigma_0 / T) \exp(E / KT), \quad (3)$$

where E_a is the activation energy for conduction, T the absolute temperature, K the Boltzmann constant and σ_0 the pre-exponential factor. The linear fit is applied for the conductivity data using least square fitting technique.

Figure 6 shows the variation of activation energy with sintering temperature. The activation energy is decreased from 1.251–0.822 eV with increase in sintering temperature.

Thus, sintering temperature affects conductivity and activation energy. With increase in sintering temperature conductivity increases and activation energy decreases. Since the doped cerias behave as pure ionic conductors in air with negligible electronic conductivity, the increased conductivity is attributed to the increase in grain interior conductivity (Xia and Liu 2002). We are now attempting to resolve this total conductivity into grain interior and grain boundary contributions.

4. Conclusions

The effect of sintering temperature on the structural, morphological and electrical properties of GDC10 was investigated. The samples sintered at and above 1673 K, showed

'fcc' structure with lattice parameter, $a = 5.418 \text{ \AA}$. Further, the surface morphology of these samples showed decreased porosity and increased uniformity. The conductivity at 800°C is of the order of $\sim 0.12 \text{ S cm}^{-1}$, which indicates that the developed material can be used as promising electrolyte for IT-SOFC.

Acknowledgements

The authors are very much thankful to DRDO for financial support. Also the authors are thankful to UGC-DAE Consortium for Scientific Research, Indore, for providing sintering facility.

References

- Brauer G and Gradinger H 1954 *Z. Anorg. Allg. Chem.* **276** 209
 Chen X J, Khor K A, Chan S H and Yu L G 2002 *Mater. Sci. Eng.* **A335** 246
 Gschneidner K A Jr 1979 *Handbook on the physics and chemistry of rare earths, non-metallic compounds* (Amsterdam: North-Holland Pub Co) Vol 3, p. 525
 Herle J V, Horita T, Kawada T, Sakai N, Yokakawa H and Dokiya M 1996 *Solid State Ionics* **86–88** 1255
 Herle J V, Horita T, Kawada T, Sakai N, Yokakawa H and Dokiya M 1997 *J. Am. Ceram. Soc.* **80** 933
 Hirano M and Kato E 1996 *Commun. Am. Ceram. Soc.* **79** 777
 Huang W, Shuk P and Greenblatt M 1997 *Solid State Ionics* **100** 23
 Mogensen M, Sammes N M and Tompett G A 2000 *Solid State Ionics* **129** 63
 Park I S, Kim S J, Lee B H and Park S 1997 *Jpn. J. Appl. Phys.* **36** 6424
 Qiu L, Ichikawa T, Hirano A, Imanishi N and Takeda Y 2003 *Solid State Ionics* **158** 55
 Sahibzada M, Steele B C H, Hellgardt K, Barth D, Effendi A, Mantzavinos D and Metcalfe I S 2000 *Chem. Eng. Sci.* **55** 3077
 Singhal S C 2000 *Solid State Ionics* **135** 305
 Song H Z, Wang H B, Zha S W, Peng D K and Meng G Y 2003 *Solid State Ionics* **156** 249
 Steele B C H 2000a *Solid State Ionics* **129** 95
 Steele B C H 2000b *Solid State Ionics* **134** 3
 Wang K, Ticky R S and Goodenough J B 1998 *J. Am. Ceram. Soc.* **81** 2565
 Xia C and Liu M 2002 *Solid State Ionics* **152** 423
 Xia C R and Liu M L 2001a *J. Am. Ceram. Soc.* **84** 1903
 Xia C R and Liu M L 2001b For GNP, provisional patent application filed
 Xia C R, Chen F L and Liu M L 2001 *Electrochem. Solid-State Lett.* **4** A52
 Zha S, Fu Q, Lang Y, Xia C and Meng G 2001a *Mater. Lett.* **47** 351
 Zha S, Xia C, Fang X, Wang H, Peng D and Meng G 2001b *Ceram. Int.* **27** 649
 Zha S W, Fu Q X, Lang Y, Xia C R and Meng G Y 2001c *Mater. Lett.* **47** 351
 Zha S, Xia C and Meng G 2003 *J. Power Sources* **115** 44
 Zhang T S, Kong L B, Zeng Z Q, Huang H T, Hing P, Xia Z T and Kilner J A 2003 *J. Solid State Electrochem.* **7** 348